

# Non-Gaussianity and direction dependent systematics in HST key project data

Shashikant Gupta<sup>1,2,3</sup> and Tarun Deep Saini<sup>2,4</sup>

<sup>1</sup> *Raman Research Institute, Bangalore, Karnataka, India, 560 080*

<sup>2</sup> *Indian Institute of Science, Bangalore, Karnataka, India, 560 012*

<sup>3</sup> *shashikant@physics.iisc.ernet.in*

<sup>4</sup> *tarun@physics.iisc.ernet.in*

30 May 2018

## ABSTRACT

Two new statistics, namely  $\Delta_\chi^2$  and  $\Delta_\chi$ , based on extreme value theory, were derived in Gupta *et al.* (2008, 2010). We use these statistics to study direction dependence in the HST key project data which provides the most precise measurement of the Hubble constant. We also study the non-Gaussianity in this data set using these statistics. Our results for  $\Delta_\chi^2$  show that the significance of direction dependent systematics is restricted to well below one  $\sigma$  confidence limit, however, presence of non-Gaussian features is subtle. On the other hand  $\Delta_\chi$  statistic, which is more sensitive to direction dependence, shows direction dependence systematics to be at slightly higher confidence level, and the presence of non-Gaussian features at a level similar to the  $\Delta_\chi^2$  statistic.

## 1 INTRODUCTION

Hubble’s observations (1929) can be approximated as  $v \propto d$ , where  $v = cz$  is the velocity (toward or away from us) of the galaxy being observed. Apart from a very few nearby galaxies, redshifts are positive indicating that the galaxies are receding away from us. The velocity of recession being proportional to its distance from us is explained by invoking the expansion of the Universe.  $H_0$ , the constant of proportionality, is called the Hubble constant and it measures the rate of expansion at the present epoch. The Hubble constant enters into various cosmological calculations and its importance can never be underestimated. It decides the value of critical density  $\rho_c$ , the amount of matter and energy required to make the geometry of the Universe flat. By comparing  $\rho_c$  to the observed density one can decide the geometry of the Universe. Most importantly it sets the age of the Universe ( $t_0$ ) and hence, size of the observable universe ( $R_{ob} = ct_0$ ). Due to its importance determining its accurate value is of paramount importance.

Accurate measurement of the Hubble constant can also lead to test the cosmological principal (CP hereafter). According to CP the universe is homogeneous and isotropic at any given cosmic epoch. If the cosmological principal is valid than one would expect the average value of Hubble constant to be same in different regions and in different directions. This issue has been addressed by various authors. We discuss some of the earlier results below.

**Are we living in a bubble?** : If the matter distribution is not homogeneous, it causes variation in the value of Hubble constant. Since gravity pulls we expect that if a region of space has higher density then the average density the expansion rate will be negatively affected and thus the Hubble

constant will be smaller in this region. In contrast to the local mass concentration a region with low mass density will produce larger value of  $H_0$ . (Zehavi *et al.* 1998) provided the first evidence for a large local void. They measured  $H_0$  within and outside  $70 h^{-1}\text{Mpc}$  using SNe Ia to find that the value of  $H_0$  was 6.5 % higher than that outside. This indicates a low density inner region compared to the outside one and is known as local bubble or Hubble bubble. The above authors had assumed a flat FRW universe with  $\Omega_M = 1$  in their analysis. The variation in the inside and outside values of  $H_0$  decreases to 4.5 % in the  $\Lambda\text{CDM}$  model ( $\Omega_M = 0.3$ ,  $\Omega_\Lambda = 0.7$ ), however, it does not disappear completely. Recently (Jha *et al.* 2007) revisited the problem using the latest SNe Ia data set and detected of the local Hubble bubble at  $3\sigma$  confidence level. However in a later publication (Conley *et al.* 2007) claimed that it was a misinterpretation of color excess of supernovae. At this juncture it is difficult to say if the evidence for the local bubble is conclusive.

**Variation in  $H_0$ , from HST key data** : (McClure & Dyer 2007) used HST Key Project data (see § 2) to calculate the variation in  $H_0$  value. The authors find that a statistically significant variation in  $H_0$  of  $9 \text{ km s}^{-1} \text{ Mpc}^{-1}$  exists in HST Key Project data. The approximate directional uncertainty is  $10^\circ$  to  $20^\circ$ . Their results indicate two sets of extrema that dominate on different distance scales. They find differences as great as  $\sim 35 \text{ km s}^{-1} \text{ Mpc}^{-1}$  within and  $\sim 20 \text{ km s}^{-1} \text{ Mpc}^{-1}$  beyond our super-cluster. Within  $70 \text{ Mpc}$  their results show a statistically significant difference of  $\sim 19 \text{ km s}^{-1} \text{ Mpc}^{-1}$ . This variation does not appear to be an artifact of Galactic dust, since there is no consistent difference looking in or out of the plane of the Galaxy. In fact, the overall structure in the map is inconsistent with the

distribution of dust in the COBE dust maps (Schlegel *et al.* 1998).

At this point one pertinent question is to ask “are these variations in the measurement of  $H_0$  due to a real departure from the cosmological principal?” On the contrary it is also possible that the data itself has some systematic errors due to some non corrected physical processes in the universe or there could be some real issues with the data reduction/calibration process. In order to comment on “what is the real cause of the variations?”, a critical review of the measurement methods is required. Measuring accurate value of the Hubble constant is a challenging task. One requires accurate measurement of redshift  $z$  and the distance  $d$ . Although redshift can be measured with good accuracy from the spectrum of the light emitted by the object, the distance measurement is difficult. Various methods are employed to measure distances, namely Tully-Fisher relation (TFR), Surface brightness (SB) fluctuations, Fundamental plane (FP) relation, SNe type II, SNe type Ia, Sunyaev-Zeldovich effect (SZE), Gravitational lensing etc. Unfortunately most of these methods suffer from the systematic effects arising from many different causes. For instance SZE requires the 3-d distribution/shape of the plasma (hot gas) in the galaxy clusters. Radio and x-ray images of the clusters provide only the projected x-ray surface brightness and CMB decrement. Hence simplified assumptions about the shape of the cluster are made. Again the assumption about the phase and the temperature of the plasma are ad hoc (Sulkanen 1999). In another example the uncertainty in the physical basis of Tully-Fisher relation can cause subtle systematic variances in the TF relation with environment. A critical review on the subject of  $H_0$  measurement methods can be found in Jacoby *et al.* (1992).

Since there are many sources of systematics, special attention was needed to measure the accurate value of  $H_0$ . The most accurate experiment to achieve this was the Hubble Space Telescope (HST) key project (Freedman *et al.* 2001). We shall discuss the HST key project in the next Section, however the issues with this data have been mentioned in previous paragraphs. In the present paper we intend to put constraints on the CP using the  $H_0$  data. This can be achieved by looking for direction dependent signatures in the data. As has been pointed out earlier detecting the direction dependent signatures does not guaranty departure from isotropy and hence CP. In that case one can constrain the reliability of the data. We use a technique (Gupta *et al.* 2008, 2010), based on extreme value theory to accomplish this. Another important issue with any data set is the presence of non-Gaussian errors. Since Central Limit Theorem (CLT) predicts that the errors in the data should be Gaussian, the non-Gaussian errors are undesired and may indicate some unresolved issues. As a by product of our method we are able to detect the presence of non-Gaussian features in the errors, which makes our methods useful not only in the case of  $H_0$  data but for any data set in general.

Plan of this paper is as follows. We discuss HST key project in § 2, which is the main source of our data. We discuss our methods in § 4. Since our techniques are based on Extreme Value Theory (EVT hereafter) we discuss it briefly in § 3. Results and conclusions are presented in § 5 and § 6 respectively.

## 2 HST KEY PROJECT AND THE DATA SET

Measuring an accurate value of  $H_0$  was one of the motivating reasons for building the NASA/ESA Hubble Space Telescope (HST). Measurement of  $H_0$  with the goal of 10% accuracy was designated as one of three “Key Projects” of the HST (Aaronson & Mould 1986; Kennicutt *et al.* 1995). The overall goal of the HST Key Project was to measure  $H_0$  based on a Cepheid calibration of a number of independent, secondary distance determination methods. Many times the systematic errors dominate the accuracy of distance measurement. To overcome this the HST team averaged over the systematics and used a number of different methods to measure distances instead of relying on a single method alone.

Determining  $H_0$  accurately requires the measurement of distances far enough away so that both the small- and large-scale motions of galaxies become small compared to the overall Hubble expansion. To extend the distance scale beyond the range of the Cepheids, a number of methods that provide relative distances were chosen. The HST Cepheid distances were used to provide an absolute distance scale for these otherwise independent methods, including the Type Ia supernovae, the Tully-Fisher relation, the fundamental plane for elliptical galaxies, surface brightness fluctuations, and Type II supernovae. The final result of HST key project (Freedman *et al.* 2001) was  $H_0 = 72 \pm 8$  km/s/Mpc.

**Data Set :** We have chosen data from the HST key project (Freedman *et al.* 2001) as our primary data set. This set contains 74 data points and provides a reasonably full sky coverage. Different methods used in order to this data set are : The TF relation, the FP relation, the SB fluctuations and SNe type Ia, SNe type II. In addition we have chosen 2 data points from (Sakai *et al.* 2000). In all the cases recessional velocities have been corrected to the CMB frame and thus all the  $H_0$  values belong to CMB frame. The full data set is published in table 1 of (McClure & Dyer 2007).

## 3 EXTREME VALUE THEORY

In the present paper we investigate the direction dependent systematic effects, which exhibit anisotropy in the cosmological data. We identify the direction where the effect of the systematics is maximum. To estimate its statistical significance we need to know the distribution of this maximum, which can be computed using Extreme Value Theory (EVT). Since it is not a common tool in the arsenal of astronomers, we begin with a brief introduction of EVT. It was developed in parallel to the Central Limit Theory (CLT). While CLT describes limiting distribution of partial sums, EVT describes how the distribution of extremes (maxima/minima) looks like. Below we discuss the theory of maxima, however, the results obtained can be easily reformulated to obtain the distribution of minima.

We shall outline the basic ingredients to obtain the theoretical distribution. Let  $F$  be a distribution with its right end point  $x^*$  which may be infinite, i.e.

$$x^* = \sup\{x : F(x) \leq 1\} .$$

We randomly choose a sample  $(X_1, X_2, \dots, X_n)$  of size  $n$  from this distribution. The maximum of this sample will approach  $x^*$  for large  $n$  i.e.  $\max(X_1, X_2, \dots, X_n) \rightarrow x^*$  as

$n \rightarrow \infty$ . The distribution of maxima has the following probability

$$\begin{aligned} & P(\max(X_1, X_2, \dots, X_n) \leq x) \\ &= P(X_1 \leq x, X_2 \leq x, \dots, X_n \leq x) \\ &= P(X_1 \leq x)P(X_2 \leq x) \cdots P(X_n \leq x) \\ &= F^n(x); \end{aligned}$$

where  $X_1, X_2, \dots, X_n$  are assumed to be independent. This converges to zero for  $x < x^*$  and to unity for  $x \geq x^*$ , which means that  $F^n(x)$  is a degenerate distribution. A normalization of variable  $\max(X_1, X_2, \dots, X_n)$  is required in order to get a non-degenerate distribution. We choose linear normalization (Haan *et al.* 2006). Let us assume that there exists a sequence  $a_n > 0$ , and  $b_n$  real such that

$$t = \frac{\max(X_1, X_2, \dots, X_n) - b_n}{a_n}$$

has a non-degenerate limiting distribution as  $n \rightarrow \infty$ , i.e.

$$\lim_{n \rightarrow \infty} F^n(a_n x + b_n) = G(x), \quad (1)$$

where  $0 \leq G(x) \leq 1$ ,  $G(x)$  is the required distribution. It is very difficult to derive the general form of  $G(x)$ , we mention some of the results available in literature. We state a theorem due to Fisher and Tippett (Fisher & Tippett 1928) which describes the required distribution.

**Theorem 1.** The distribution of maxima  $G(x; \varepsilon)$  has the following form :

$$G(x; \varepsilon) = \exp\left(-[1 + \varepsilon x]^{-1/\varepsilon}\right), \quad (2)$$

with  $1 + \varepsilon x > 0$ . Where  $\varepsilon R$  is called the shape parameter or the extreme value index.

Proof of this theorem (Fisher & Tippett 1928) is beyond the scope of this paper. We only outline a few interesting facts :

- When  $\varepsilon = 0$  :

Taylor expansion of  $[1 + \varepsilon x]^{-1/\varepsilon}$  gives  $e^{-x}$ . Thus Eq 2 gives

$$G(x) = \exp(-e^{-x}).$$

This is known as the Gumbel distribution or extreme value distribution of type I. The right end point of this distribution is infinity. Also  $1 - G(x) \sim e^{-x}$  as  $x \rightarrow \infty$ , indicating that the distribution has a thin tail. It is clear from the form of Gumbel that it is unbounded on either side that is, there is no  $x$  for which  $G(x) = 0$ . A sketch of Gumbel distribution is shown in Fig 1.

- When  $\varepsilon > 0$  :

$G(x; \varepsilon) < 1$  for all  $x$ , i.e. the right end point of the distribution is infinity. Also as  $x \rightarrow \infty$ ,  $1 - G(x, \varepsilon) \sim (\varepsilon x)^{-1/\varepsilon}$ . Which indicates that the distribution has a heavy tail. This is called Frchet distribution, or type II extreme value distribution. One can clearly see that this distribution has a lower bound.

- When  $\varepsilon < 0$  :

The right end point of the distribution is  $-1/\varepsilon$ . This is known as Weibull distribution, or extreme value distribution of type III.

In the above discussion we have not mentioned the location and scale parameters for simplicity. When we introduce

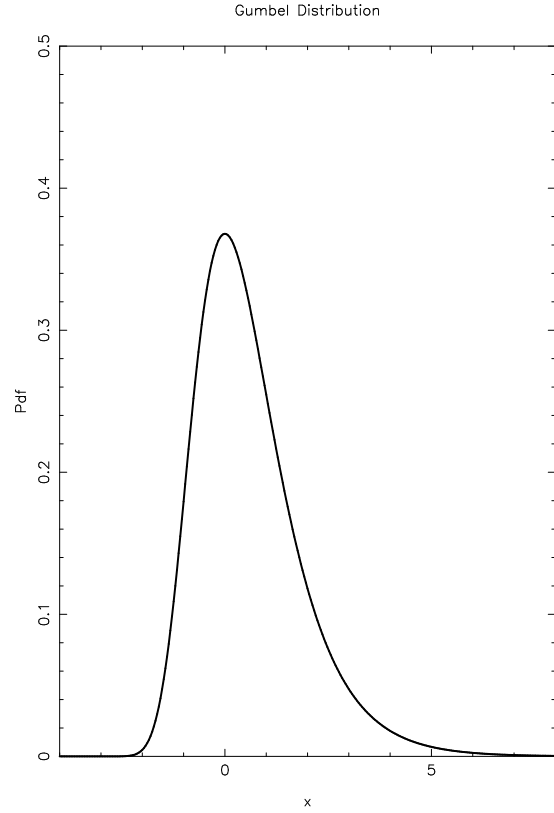


**Figure 1.** A sketch of Gumbel distribution. Here we have plotted the probability distribution function which is derivative of  $G(x)$ .

these parameters, the form of  $G(x)$  becomes complicated as shown below

$$G(x; m, s, \varepsilon) = \exp\left(-\left[1 + \varepsilon\left(\frac{x-m}{s}\right)\right]^{-1/\varepsilon}\right), \quad (3)$$

where  $m = b_n \in R$  is the location parameter and  $s = a_n > 0$  is the scale parameter.

For our analysis we shall use the Gumbel distribution since the variable of interest there does not have bound on either side. Thus our emphasis will be on the Gumbel distribution in the rest of this paper, which with scale and location parameters takes the form

$$G(x; m, s) = \exp\left(-\left[\exp\left(-\frac{x-m}{s}\right)\right]\right), \quad (4)$$

The probability distribution (pdf) can be derived by differentiating Eq 4.

## 4 METHODOLOGY

Two new techniques, namely  $\Delta_{x^2}$  and  $\Delta_x$  statistics based on Extreme value theory, were derived in Gupta *et al.* (2008, 2010). We apply the same method here, however we briefly mention these techniques for completeness.

#### 4.1 $\Delta_{\chi^2}$ statistic

First we calculate the best fit value of  $H_0$  for the *complete data set* by minimizing  $\chi^2$ , defined below

$$\chi^2 = \sum_i \left( \frac{H_{0i} - H_0}{\sigma_i} \right)^2, \quad (5)$$

where  $H_{0i}$  is the  $i^{th}$  point in the data set and  $\sigma_i$  is the observed standard error. This minimization gives us the best fit value  $H_{0b}$ .

Using this best fit value we now define  $\chi_i$  for the  $i^{th}$  data point as

$$\chi_i = \frac{H_{0i} - H_{0b}}{\sigma_i}, \quad (6)$$

where  $H_{0b}$  is the best fit value of the Hubble constant. We shall consider subsets of the data set to construct our statistic. We define the reduced  $\chi^2$  in terms of  $\chi_i$  as follows

$$\chi^2 = \frac{1}{N_{\text{subset}}} \sum_i \chi_i^2, \quad (7)$$

where it should be noted that by ‘reduced’ we do not mean ‘per degree of freedom’, since we *do not fit* the model separately to the subsets of the data. Here  $\chi^2$  is an indicator of the statistical scatter of the subset from the best fit value  $H_{0b}$ .

If the Cosmological Principle holds then the value of the Hubble constant should not depend upon the direction in which it is measured. We use this fact to choose specific subsets of data. We divide the complete data into two hemispheres, labeled by the direction vector  $\hat{n}_i$ , and take the difference of the reduced  $\chi^2$  computed for the two hemispheres separately to obtain  $\Delta\chi_{\hat{n}_i}^2 = \chi_{\text{north}}^2 - \chi_{\text{south}}^2$ , where we have defined ‘north’ as that hemisphere towards which the direction vector  $\hat{n}_i$  points. We are only interested in the magnitude of this difference, therefore, we take the absolute value of  $\Delta\chi_{\hat{n}_i}^2$ , and then vary the direction  $\hat{n}$  across the sky to obtain the maximum absolute difference

$$\Delta_{\chi^2} = \max\{|\Delta\chi_{\hat{n}_i}^2|\}. \quad (8)$$

We note that since the same data point appears in several subsets, the maximization is not done over statistically independent measures of our statistic. Another noteworthy fact is that if the direction dependence has a forward-backward symmetry then this statistic will not be able to detect it. However, due to its ease of construction and use we consider this simplest of possible statistics.

To interpret our results we need to know the range of  $\Delta_{\chi^2}$  that we can expect if there were no direction dependence in data, and the noise in the measurements were Gaussian. The spatial distribution of measurements is not uniform on the sky, therefore, the number of measurements in the two hemispheres, for a given direction, varies with the direction  $\hat{n}$  in a complicated manner. Therefore one might expect the probability distribution function  $P(\Delta_{\chi^2})$  to be extremely complicated, however, extreme value theory, § 3, shows that the distribution is, in fact, a simple, two parameter Gumbel distribution, characteristic of extreme value distribution type I:

$$P(\Delta_{\chi^2}) = \frac{1}{s} \exp \left[ -\frac{\Delta_{\chi^2} - m}{s} \right] \exp \left[ -\exp \left( -\frac{\Delta_{\chi^2} - m}{s} \right) \right], \quad (9)$$

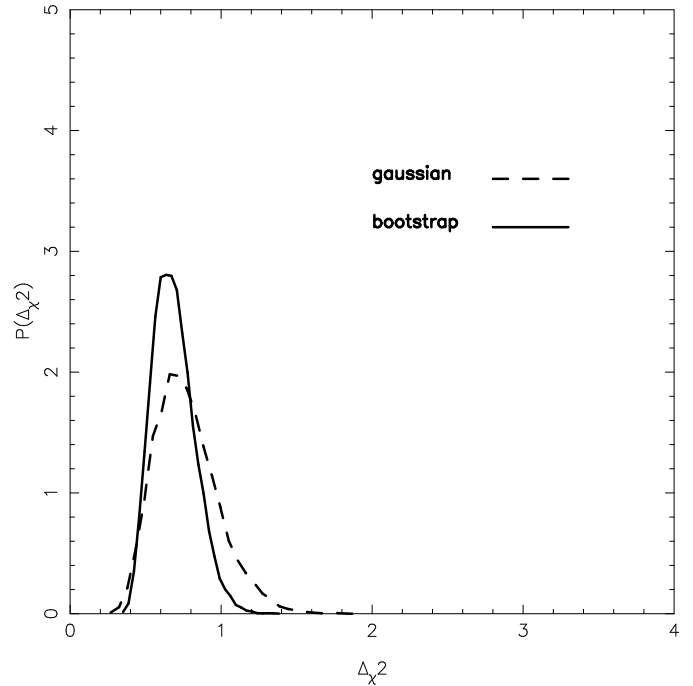


**Figure 2.** Here we plot the probability density of  $\Delta_{\chi^2}$  for the simulated data. Solid curve represents the bootstrap distribution while broken curve represents the theoretical distribution assuming Gaussian errors.

where the position parameter  $m$  and the scale parameter  $s$  completely determine the distribution.

To quantify departures from isotropy we need to know the theoretical distribution  $P_{\text{theory}}(\Delta_{\chi^2})$ . Even though we know what to expect in a general manner, it is difficult to obtain the parameters  $s$  and  $m$  analytically, therefore, we calculate this distribution numerically by simulating several sets of Gaussian distributed  $\chi_i$  on the measurement positions and obtaining  $\Delta_{\chi^2}$  from each realization.

If the noise in the data is Gaussian then the above distribution adequately quantifies the directional dependence in the data. But if the data has non-Gaussian noise then the theoretical distribution cannot be used to quantify the level of significance of our possible discovery of anisotropy. We construct an independent test for directional dependence by obtaining the bootstrap distribution  $P_{\text{BS}}(\Delta_{\chi^2})$ , which is constructed in the following manner. The observed  $\chi_i$ 's are assumed to be drawn from some unknown, direction dependent probability distribution. We shuffle the data values  $H_{0i}$  and  $\sigma_i$  over the measurement positions, thus destroying any directional alignment they might have had due to anisotropy. Thus we are able to generate several realizations of data and estimate the distribution  $P_{\text{BS}}(\Delta_{\chi^2})$ .

In order to know what to expect from this statistic we simulate data and calculate the above mentioned Bootstrap and numerical distributions. These are shown in Fig. 2. As had been discussed in (Gupta *et al.* 2010) there exists a specific bias between the two distributions. Since the numerical distribution is obtained by assuming  $\chi_i$ 's to be Gaussian random variates with a zero mean and unit variance, therefore, it does not have any bounds. However the bootstrap distribution is obtained by shuffling through a *specific realization*

of  $\chi_i$  where the  $\chi_i$ s are obviously bounded. It is clear that on the average this should produce slightly smaller values of  $\Delta_{\chi^2}$  in comparison to what one expects from a Gaussian distributed  $\chi_i$ s.

Our results for  $\Delta_{\chi^2}$  statistic in this paper should be interpreted with respect to Figure 2. Concerns regarding the small number of data points in data set and its effect on the efficacy of our method can be addressed (as in Gupta *et al.* (2010)) by noting that this figure is produced with only 76 points and the theoretical and the bootstrap distributions look similar.

#### 4.2 $\Delta_{\chi}$ statistic

As mentioned above,  $\chi_i^2$  does not contain information about whether the measurement is above or below the fit i.e. greater or smaller than  $H_{0b}$ . An obvious generalization that does contain this information can be obtained by considering a statistic based on  $\chi_i$ s. We consider two subsets of data defined by two hemispheres labeled by the direction vector  $\hat{n}$ , containing  $N_{\text{north}}$  and  $N_{\text{south}}$  data points, where the total number of data points,  $N = N_{\text{north}} + N_{\text{south}}$ , and define the quantity

$$\Delta_{\chi_{\hat{n}}} = \frac{1}{\sqrt{N}} \left( \sum_{i=1}^{N_{\text{north}}} \frac{\chi_i}{\sigma_i} - \sum_{j=1}^{N_{\text{south}}} \frac{\chi_j}{\sigma_j} \right). \quad (10)$$

Clearly  $\langle \Delta_{\chi_{\hat{n}}} \rangle = 0$  and  $\langle (\Delta_{\chi_{\hat{n}}})^2 \rangle = 1$ . From the central limit theorem (Kendall & Stuart 1977) it follows that for  $N \gg 1$ , the quantity  $\Delta_{\chi}$  follows a Gaussian distribution with a zero mean and unit variance. As in the previous case we maximize this quantity by varying the direction  $\hat{n}$  across the sky to obtain the maximum absolute difference

$$\Delta_{\chi} = \max\{|\Delta_{\chi_{\hat{n}}}| \}. \quad (11)$$

This statistic differs from the previous one in that the  $\Delta_{\chi}$  statistic has a theoretical limit where the position and the shape parameters can be determined analytically. Given  $N_d$  independent directions on the sky we are essentially determining the maximum of a sample of size  $N_d$  where the individual numbers are drawn from a Gaussian distribution with a zero mean and unit variance. In the limit  $N_d \gg 1$  the parameters are given by (Haan *et al.* 2006)

$$m = \sqrt{2 \log N_d - \log \log N_d - \log 4\pi} \quad (12)$$

$$s = \frac{1}{m} \quad (13)$$

where we have to additionally assume that the number of measurements  $N \gg 1$ , since the distribution for  $\chi$  becomes Gaussian only in this limit. This is convenient since at least for large data sets, which will be available in the future, a comparison with theory becomes simpler. However, for a smaller number of measurements (data points) there is a possibility that not all directions are independent, in fact, it is quite possible that two directions contain exactly same subsets in the two hemisphere. In this situation it is clear that the total independent directions is a smaller number than  $N_d$  and thus theoretical distribution would be rightward shifted and also more sharply peaked. For this reason we also calculate the bootstrap distribution and the theoretical distribution in the same manner as for the previous statistic.

**Table 1.** Best fit value for  $H_0$

Best fit	$\chi^2$	$\chi^2_{\text{per dof}}$
72.0	194.1	2.6

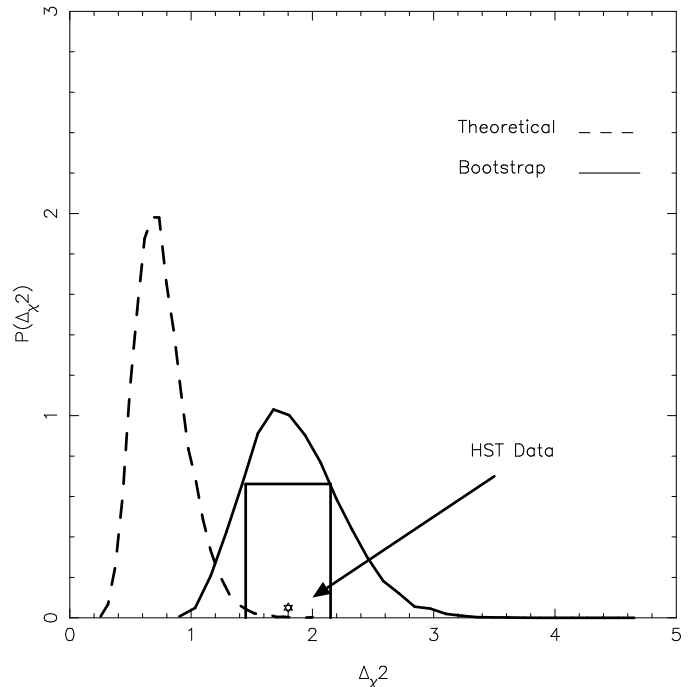


**Figure 3.** Here we plot the probability density of  $\Delta_{\chi^2}$ . Solid curve represents the bootstrap distribution while broken curve represents the theoretical distribution assuming Gaussian errors. The two curves do not match.  $\Delta_{\chi^2}$  for the data lies close to the peak of bootstrap distribution.

## 5 RESULTS

First we obtain the best fit value,  $H_{0b}$ , of the Hubble constant for the data, which is shown in Table 1. The large value of  $\chi^2$  suggests that the error bars may have been underestimated.

**$\Delta_{\chi^2}$  statistic :** We have applied the  $\Delta_{\chi^2}$  statistic to this data and calculated the bootstrap and theoretical distributions for the HST Key Project data, as discussed earlier. The theoretical and bootstrap distributions for this data are shown in Fig 3. To interpret our results we compare with Fig 2. We see that the Theoretical distribution has been shifted far away on the left side of the bootstrap distribution. This contradicts to the fact that bootstrap distribution should lie slightly to the left of the theoretical distribution, as explained above, indicating the non-Gaussian nature of errors in the data. HST Key data lies outside the theoretical distribution, but is close to the peak of the bootstrap distribution. This suggests that either the data is free from direction dependent systematics or a more sensitive technique is required to put constraints on these systematics.

#### $\Delta_{\chi}$ statistic :

We apply  $\Delta_{\chi}$  statistic to the data and calculate the bootstrap and numerical distributions. These are shown in

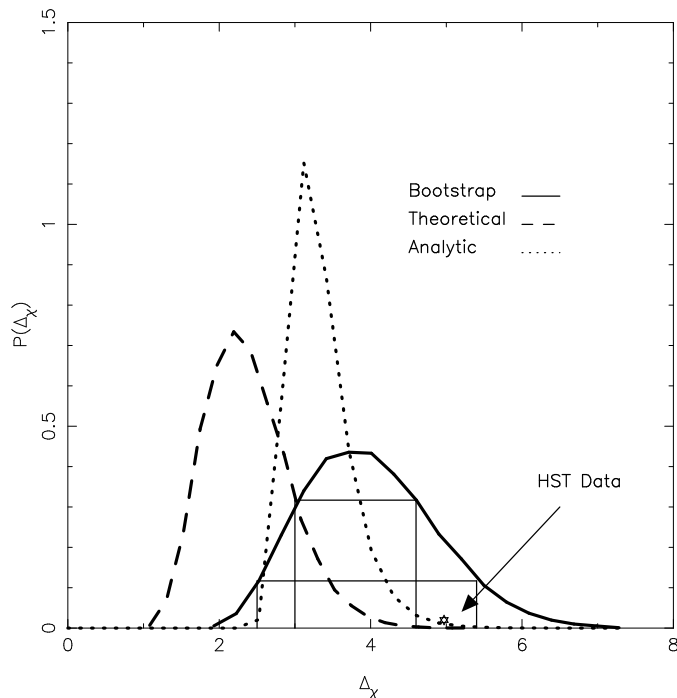


**Figure 4.** Here we plot the probability density of  $\Delta_\chi$ . Solid curve represents the bootstrap distribution while broken curve represents the numerically calculated distribution assuming Gaussian errors. The two curves do not match very well. The analytically calculated distribution is shown by dotted lines.  $\Delta_\chi$  for the HST key data lies outside one  $\sigma$  region around the peak of bootstrap distribution.

Fig 4. Here also the numerical distribution lies to the left of the bootstrap distribution, which is in contradiction to the expected relative positions of the two. Interestingly, in this case we have an advantage, since we can calculate the theoretical distribution analytically. This analytic distribution is shown by dotted line in Fig 4. It was discussed in § 4.2 that if all the directions are not independent then the analytic distribution should lie on the right side of the numerical distribution and should be peaked sharply. This is what we observe in Fig 4. Bootstrap distribution lies to the right of the analytic distribution, however, we find that it is wider than what we would expect from a true Gumbel distribution. This indicates that the bootstrap distribution is not truly Gumbel, therefore, it should be compared with the numerical distribution, which is calculated in a manner that is identical to the bootstrap one. Comparison shows that the two distributions differ in a manner identical to the difference seen in Fig 3, based on the  $\Delta_{\chi^2}$  statistic; indicating a similar level of non-Gaussianity. We also find that the position of the data lies outside the  $1\sigma$  region from the peak of the bootstrap distribution.

## 6 CONCLUSIONS

We have applied the  $\Delta_{\chi^2}$  and  $\Delta_\chi$  statistics to the HST Key Project data. We find that in both the cases the bootstrap and the theoretical distributions are very different from each other. Thus we conclude that the nature of the errors in the data is non-Gaussian.  $\Delta_{\chi^2}$  statistic does not show direction

dependence in the data, however,  $\Delta_\chi$  statistic which is more sensitive to the direction dependence, shows the presence of direction dependent systematics at around one  $\sigma$  level.

**Acknowledgements** Shashikant thanks Arnab Rai Chodhuri for supporting part of this work by his DST grant (DST0815).

## REFERENCES

- Aaronson, M., & Mould, J. 1986, *Astroph. J.* , 303, 1.  
 Conley, A., Carlberg, R. G., Guy, J., Howell, D. A., Jha, S., Riess, A. G., & Sullivan, M. 2007, *Astroph. J. Lett.* , 664, L13.  
 Fisher, R. A. and Tippett, L.H.C. , *Proc. Cambridge Philos. Soc.* 1928, 24, 180.  
 Freedman, W. L., Madore, B. F., Gibson, B. K., *et al.*, 2001. *ApJ*, 553, 47.  
 Gupta, Shashikant, Saini, Tarun, Deep, Laskar, Tanmoy, 2008 *Mon. Not. Roy. Ast. Soc.* 388, 242.  
 Gupta, Shashikant, Saini, Tarun, Deep, 2010 *Mon. Not. Roy. Ast. Soc.* 407, 651.  
 Haan L. and Ferreira A., “Extreme Value Theory: An Introduction” Springer 2006.  
 Jacoby, G. H., *et al.* 1992, *Pub. Astro. Soc. Pacific* , 104, 599  
 Kendall, M., & Stuart, A. 1977, London: Griffin, 1977, 4th ed.,  
 Jha, S., Riess, A., G. and Kirshner, R., P., 2007, *Astroph. J.* , 659, 122.  
 Kennicutt, R. C., Jr., Freedman, W. L., & Mould, J. R. 1995, *Astron. J.* , 110, 1476.  
 McClure, M. L., & Dyer, C. C. 2007, *New Astronomy* , 12, 533.  
 Sakai, S., Mould, J. R., Hughes, S. M. G., *et al.*, 2000. *ApJ*, 529, 698.  
 Schlegel, D. J., Finkbeiner, D. P., Davis, M., 1998. *ApJ*, 500, 525.  
 Sulkanen, M. E. 1999, *Astroph. J.* , 522, 59.  
 Zehavi I., Riess A. G., Kirshner R. P., Dekel, A., 1998, *Astroph. J.* 503, 483.